NIH Public Access
Author Manuscript
Cell Calcium. Author manuscript; available in PMC 2015 August 01.

Published in final edited form as:
Cell Calcium. 2014 August ; 56(2): 96–107. doi:10.1016/j.ceca.2014.05.004.

Characterization of Ryanodine Receptor Type 1 Single Channel Activity Using "On-Nucleus" Patch Clamp

Larry E. Wagner II, **Linda A. Groom**, **Robert T. Dirksen**, and **David I. Yule***
Department of Pharmacology and Physiology, University of Rochester, 601 Elmwood Ave, Rochester. NY 14642

Abstract

In this study, we provide the first description of the biophysical and pharmacological properties of ryanodine receptor type 1 (RyR1) expressed in a native membrane using the on-nucleus configuration of the patch clamp technique. A stable cell line expressing rabbit RyR1 was established (HEK-RyR1) using the FLP-in 293 cell system. In contrast to untransfected cells, RyR1 expression was readily demonstrated by immunoblotting and immunocytochemistry in HEK-RyR1 cells. In addition, the RyR1 agonists 4-CMC and caffeine activated Ca^{2+} release that was inhibited by high concentrations of ryanodine. On nucleus patch clamp was performed in nuclei prepared from HEK-RyR1 cells. Raising the [Ca^{2+}] in the patch pipette resulted in the appearance of a large conductance cation channel with well resolved kinetics and the absence of prominent subconductance states. Current versus voltage relationships were ohmic and revealed a chord conductance of ~750 pS or 450 pS in symmetrical 250 mM KCl or CsCl, respectively. The channel activity was markedly enhanced by caffeine and exposure to ryanodine resulted in the appearance of a subconductance state with a conductance ~40 % of the full channel opening with a P_o near unity. In total, these properties are entirely consistent with RyR1 channel activity. Exposure of RyR1 channels to cyclic ADP ribose (cADPr), nicotinic acid adenine dinucleotide phosphate (NAADP) or dantrolene did not alter the single channel activity stimulated by Ca^{2+}, and thus, it is unlikely these molecules directly modulate RyR1 channel activity. In summary, we describe an experimental platform to monitor the single channel properties of RyR channels. We envision that this system will be influential in characterizing disease-associated RyR mutations and the molecular determinants of RyR channel modulation.

Keywords

Ryanodine Receptor; Inositol 1,4,5-trisphosphate Receptor; Single channel Measurement

© 2014 Elsevier Ltd. All rights reserved.

*Correspondence: David_Yule@urmc.rochester.edu; Tel, 585-273-2154.

Publisher's Disclaimer: This is a PDF file of an unedited manuscript that has been accepted for publication. As a service to our customers we are providing this early version of the manuscript. The manuscript will undergo copyediting, typesetting, and review of the resulting proof before it is published in its final citable form. Please note that during the production process errors may be discovered which could affect the content, and all legal disclaimers that apply to the journal pertain.

NIH-PA Author Manuscript
NIH-PA Author Manuscript
NIH-PA Author Manuscript

NIH-PA Author Manuscript
NIH-PA Author Manuscript
NIH-PA Author Manuscript

1. Introduction

Ryanodine receptors (RyR) and inositol 1,4,5-trisphosphate receptors (IP_3R) are the principle intracellular Ca^{2+} release channels resident in the sarcoplasmic reticulum (SR) and endoplasmic (ER), respectively [1]. The proteins share many key structural and functional features [2–4]. In particular, each protein family is encoded by three distinct genes, the proteins exhibit a similar domain structure, and when assembled, result in large conductance, tetrameric Ca^{2+}-permeable cation channels [3–6]. The conserved organization across these channels [7–10] is best illustrated by the observation that some structurally analogous domains of the IP_3R and RyR are functionally interchangeable when heterologously expressed as chimeric receptors [11]. Furthermore, the individual channel subtypes are often expressed with a specific tissue and cellular distribution and this, together with subtype-specific regulation of Ca^{2+} release by various modulatory factors and events, play major roles in defining the diversity and specificity of intracellular Ca^{2+} signals [5, 12, 13]. As such, Ca^{2+} release through IP_3R and RyR channels controls a diverse array of physiological processes including muscle contraction, exocytosis, cell-fate and gene transcription [1, 14, 15].

Typically, the properties, regulation and function of intracellular Ca^{2+} release channels are studied either by monitoring cytosolic Ca^{2+} signals or by electrophysiological techniques [5, 6, 16]. While the former methods are very convenient and have provided a wealth of important information, the cytosolic Ca^{2+} signal is only an indirect measure of release channel activity, is often not kinetically resolved, and does not yield definitive biophysical information regarding ion channel gating and permeation. Incorporation of both RyR and IP_3R into planar lipid bilayers has been the predominant approach used in the field to directly characterize the regulation, pharmacology, and biophysical properties (e.g. conductance, permeation, and gating) of IP_3R and RyR channels [17–19]. Nevertheless, common criticisms of bilayer measurements are that the channels are not studied in native membranes and important regulatory factors may be absent. Thus, the degree to which bilayer data accurately reflects channel behavior *in situ* is difficult to gauge. An obvious barrier to conventional electrophysiological study of native RyRs and IP_3Rs is their distribution to sub-cellular membrane compartments, which are clearly not easily amenable to patch clamp measurements. Circumventing this problem, a few studies have demonstrated that a small proportion of IP_3R and RyRs are present in the plasma membrane of some cell types, and therefore, can be studied using conventional patch clamp techniques [20–22]. However, while these channels are resident in a biologically relevant membrane, interpretation is complicated as the channels are not investigated in the specific context of the lipid and protein environment of the ER/SR and are not subjected to regulation by luminal ER/SR factors.

A significant technical advance, which largely negates the confounding issues associated with the former approaches, has been the development of “on-nucleus” patch clamp recordings of intracellular IP_3R channels [6, 23–28]. In this paradigm, single channel activity is recorded following attaining a giga-ohm seal on the outer nuclear envelope or associated contiguous ER membrane from a nucleus extracted from a cell expressing the channel of interest. To date, these methods [29], used almost exclusively to study IP_3R, have

NIH-PA Author Manuscript

NIH-PA Author Manuscript

NIH-PA Author Manuscript

yielded important information defining the fundamental single channel properties of IP_3R subtypes operating within their native environment together with mechanistic information regarding regulation of the channels by important co-agonists and cellular factors [30–32]. While these techniques have not been applied to RyR in any systematic manner, they are clearly also applicable to the study of this channel and have the potential to yield novel information relating to the gating, permeation and regulation of native and disease-associated mutant RyR channels. Thus, as proof of principle, here we provide the first biophysical and pharmacological characterization of the single channel activity of the skeletal muscle type-1 RyR (RyR1) heterologously expressed in a native intracellular membrane.

2. Methods

2.1 Generation of RyR1 stable expressing cell line

A rabbit RyR1 cDNA was cloned into the NheI site of pcDNA5/FRT (RyR1-pcDNA5/FRT) and verified by sequencing. The clone was then used to generate a stable cell line using the Flp-In™ System (Invitrogen, Grand Island, NY). A 60 mm dish of Flp-In™ 293 host cells was transfected with 2 μg of RyR1-pcDNA5/FRT and 9 μg of the Flp recombinase expression vector (pOG44) using 4 μl of Lipofectamine 2000. The next day, selection was started using 100 ug/ml Hygromycin B. Stable clones were then expanded and frozen. RyR1 protein expression was assayed by immunocytochemistry and immunoblot.

2.2 RyR1 western blot analysis

Cells stably expressing RyR1 (HEK-RyR1) and control Flp-In 293 cells were washed 3 times with cold 1 X PBS. Cells were lysed in cold RIPA buffer (50 mM Tris-HCL, 150 mM NaCl, 1% NP-40, 0.25% sodium deoxycholate, pH 7.4) plus protease inhibitors (Complete Protease Inhibitor Tablets, Roche, Basel, Switzerland). Cell debris was removed by centrifugation (13,000 x g) at 4°C for 15 min and the supernatant collected. Proteins were separated by SDS-PAGE on 4.5% (RyR1) or 15% (FKBP) gels and then electrophoretically transferred to nitrocellulose membrane. The membrane was blocked for 1 h at room temperature with 5% milk in a Tris-buffered saline containing 0.15% Tween 20 (TBST). Membranes were incubated with either anti-RyR (34C, 1:30; Developmental Studies Hybridoma Bank, University of Iowa, Iowa City, IA) or anti-FKBP12 (N-19, 1:100; Santa Cruz, Dallas, Texas) primary antibodies overnight at 4°C in 5% milk/TBST. Membranes were then washed 3 times with TBST and incubated in the dark with either secondary anti-mouse IgG (H+L) DyLight 800 conjugated antibody (for RyR, 1:10,000, Thermo Scientific, USA) or anti-goat IgG (H+L) DyLight 800 conjugated antibody (for FKBP, 1:10,000, Thermo Scientific, USA) for 1 h in 5% milk/TBST. An Odyssey infrared imaging system (LI-COR Biosciences, Lincoln, NE, USA) was used to detect bound antibody.

2.3 Immunofluorescence imaging

HEK-RyR1 and control Flp-In 293 cells plated on glass cover slips were fixed with 4% paraformaldehyde in PBS for 20 min. Nuclei were stained by incubation with 2 μg/ml Hoechst 34580 (Molecular Probes, Grand Island, NY) for 15 min. Cells were immunostained with 34C mouse monoclonal anti-RyR (1:30) antibody overnight at 4°C, as

NIH-PA Author Manuscript

NIH-PA Author Manuscript

NIH-PA Author Manuscript

previously described [33]. The following day, cover slips were washed with PBS 3 times (5 min) and then incubated for 1 h at room temperature in blocking buffer containing a 1:500 dilution of rhodamine-labeled goat anti-mouse IgG (Jackson ImmunoResearch Laboratories Inc., West Grove, PA). Cover slips were then washed 3 times with PBS and mounted on glass slides. All confocal images were obtained using an Olympus Fluoview 1000MP confocal microscope equipped with a suite of gas and diode lasers.

2.4 Measurements of agonist-induced Ca^{2+} release in HEK-RyR1 and control Flp-In 293 cells

HEK-RyR1 and control Flp-In 293 cells plated on cover slips were loaded with 6 μM indo-1 AM (TefLabs Inc., Austin, TX) for 30 min at 37°C. Cells were then bathed in dye-free Ringer's solution (in mM: 145 NaCl, 5 KCl, 2 $CaCl_2$, 1 $MgCl_2$, 10 HEPES, pH 7.4) and placed on the stage of an inverted epifluorescence microscope (Nikon Instruments, Melville, NY). Cytosolic dye within a small rectangular region of the cell was excited at 350 ± 10 nm and fluorescence emission at 405 ± 30 nm (F_{405}) and 485 ± 25 nm (F_{485}) was recorded using a photomultiplier based detection system (Photon Technologies Inc., Birmingham, NJ). Results were presented as the ratio of F_{405} and F_{485} ($R = F_{405}/F_{485}$). A standard protocol was used to measure RyR1-releasable Ca^{2+} content, which included sequential 30 second local perfusions of control Ringer's solution, either 10 mM caffeine or 500 μM 4-chloro-m-cresol (4-CMC), and finally, washout with control Ringer's. In experiments to block RyR-mediated Ca^{2+} release, HEK-RyR1 cells were pretreated with 100 μM ryanodine for 30 min prior to the addition of 10 mM caffeine. Relative changes in intracellular Ca^{2+} were reported as the maximum change in indo-1 ratio ($\Delta Ratio = R_{agonist} - R_{baseline}$) observed during agonist application. Data are presented as mean ± SEM with significance accepted at $P < 0.001$ (unpaired Student's *t* test). 4-CMC concentration-response curves were obtained by monitoring the peak ΔRatio at each [4-CMC] following sequential exposure of HEK-RyR1 and control Flp-In 293 cells to increasing concentrations of 4-CMC (1, 5, 20, 100, 500 μM) applied using a rapid (less than 5 second response time) local perfusion system (Warner Instrument Corp., Hamden, CT).

2.5 Preparation and isolation of nuclei

Isolated HEK-RyR1 nuclei were prepared by homogenization. Homogenization buffer (HB) contained 250 mM sucrose, 150 mM KCl, 1.4 mM β-mercaptoethanol, 10 mM Tris, pH 7.3. A complete protease inhibitor tablet (Roche, USA) was added subsequent to pH adjustments. Cells were washed and re-suspended in HB prior to nuclear isolation using a RZR 2021 homogenizer (Heidolph Instruments, Germany) with 8 strokes at 1200 RPM. 3 μl of nuclear suspension were placed in 3 ml of bath solution (BS) containing: 250 mM KCl, 25 mM HEPES, 500 μM BAPTA, and 180 μM $CaCl_2$ (~200 nM free Ca^{2+}), pH 7.3. The bath solution used in Ca^{2+} uncaging experiments contained no added Ca^{2+} or chelator. Nuclei were allowed to adhere to a plastic culture dish for 10 minutes prior to electrophysiological experimentation.

NIH-PA Author Manuscript

NIH-PA Author Manuscript

NIH-PA Author Manuscript

2.6 Single RyR1 channel measurements in isolated HEK-RyR1 nuclei

Single RyR1 channel potassium currents (i_k) were measured in the on-nucleus patch clamp configuration using PClamp 9 and an Axopatch 200B amplifier (Molecular Devices, Sunnydale, California). The patch pipette (cytosolic) solution contained 250 mM KCl, 25 mM HEPES, 500 μM ATP with varying concentrations of $CaCl_2$, and 5,5′-dibromo BAPTA for a free [Ca^{2+}] between 600 nM and 4 μM, pH 7.3. Pipette resistances were typically between 10 and 20 MOhms and seal resistances were >5 GOhms. Ca^{2+} chelators were not used for free [Ca^{2+}] ≥100 μM. Free [Ca^{2+}] was estimated using MaxChelator (http://maxchelator.stanford.edu/) and verified fluorometrically. For Ca^{2+} uncaging experiments, the pipette solution contained 250 mM KCl, 25 mM HEPES, 500 μM Na_2ATP, 10 mM NP-EGTA, and 3 mM $CaCl_2$ (free [Ca^{2+}] was approximately 100 nM). Ca^{2+} was liberated from NP-EGTA using UV flash photolysis. Free [Ca^{2+}] following UV release was unknown, but was likely greater than 10 μM. Solutions containing nicotinic acid adenine dinucleotide phosphate (NAADP) and cyclic ADP-ribose (cADPR) were added directly into the patch pipette solution (containing 1 μM Ca^{2+}), while caffeine, ryanodine and dantrolene were dissolved in bath solution for direct perfusion of nuclei. Solutions were superfused by gravity through a multi-barrel perfusion pipette of our own design that was placed immediately adjacent to the nucleus [32]. Due to the design of the perfusion pipette, there was very little dead space allowing rapid solution exchanges. Traces shown reflect consecutive 3 second sweeps recorded at 40 mV, sampled at 20 kHz and filtered at 5 kHz. A minimum of 15 seconds of continuous recording was used for data analyses.

2.7 Data analysis

Single channel openings were detected using a 50% threshold crossing criterion utilizing the event detection protocol in Clampfit 9. We assumed that the number of channels in any particular patch is represented by the maximum number of discrete stacked events observed during the experiment. Only patches with 1 apparent channel were considered for analyses. The probability of opening (P_o), unitary current amplitude (i_k), open and closed times, and burst analyses were calculated using Clampfit 9 and Origin 6 software (Origin Lab, Northampton, Massachusetts). All-points current amplitude histograms were generated from the current records and fitted using a normal Gaussian probability distribution function. The coefficient of determination (R^2) for every fit was > 0.95. The P_o was calculated using the multimodal distribution for the open and closed current levels. Channel dwell time constants for the open and closed states were determined from exponential fitting of binned open and closed dwell time histograms. The threshold for an open event was set at 50% of the maximum open current and events shorter than 0.1 ms were ignored. Slope conductances were determined from linear fitting of current–voltage relationships using the following equation:

$$g_k = i_k/(V - V_k)$$

Where g_k is the unitary potassium conductance, i_k is unitary potassium current, V is test voltage, and V_k is the potassium reversal potential. Equation parameters were estimated

NIH-PA Author Manuscript

NIH-PA Author Manuscript

NIH-PA Author Manuscript

using a non-linear, least squares fitting algorithm. Two tailed heteroscedastic *t* tests with *P*-values < 0.05 were considered to have statistical significance.

3. Results

3.1 Stable expression of RyR1 results in ER localization of functional channels

IP_3R single channel activity has been successfully recorded in outer nuclear/ER membranes isolated from a variety of cells [6]. Examples include endogenous, native receptors, together with channels present following heterologous expression. A particularly powerful experimental paradigm utilizes stable IP_3R expression in the DT40-3KO, IP_3R-*null*, chicken pre B lymphocyte cell line [32]. This system has been used extensively to monitor the activity of a variety of wild-type IP_3R subtypes and mutants without the interpretation of data being confounded by the presence of endogenous channels. We reasoned that a similar general approach of expression of RyR on a null background might provide an appropriate framework for studying RyR single channel activity. We therefore chose to establish HEK-293 cells stably expressing RyR1. Stable cell lines were generated using the Flp-In system as described in Methods. Western blotting and immunocytochemistry were performed to confirm RyR expression and appropriate subcellular localization. As shown in Figure 1A, a band of appropriate molecular weight (~538 kDa) was detected by α-RyR antisera in lysates prepared from HEK293-FLP-In cells stably expressing wild type rabbit RyR1 (HEK-RyR1) and from a SR preparation of mouse skeletal muscle, but not from control Flp-In 293 cells. In addition, western blots also demonstrated the endogenous expression of the RyR accessory protein, FK-506 binding protein (FKBP) (Figure 1B). Similarly, confocal microscopy performed in fixed cells using α-RyR antisera clearly detected protein only in HEK-RyR1 cells (compare Figure 1 C(I) and C(II)), which exhibited a highly reticular distribution consistent with expression of RyR1 in the ER of HEK-RyR1 cells (Figure 1C(III)).

Next, experiments were performed to establish that the expressed RyR1 formed functionally competent Ca^{2+} release channels. Indo-1 loaded HEK-RyR1 and control Flp-In 293 cells were exposed to sequential 30 seconds additions of various concentrations of the RyR1 agonist, 4-chloro-*m*-cresol [34] (4-CMC) (1, 5, 20, 100 and 500 μM) followed by a 30-second wash in control buffer. As shown in the representative trace in Figure 2A, HEK-RyR1 cells (red trace) exposed to a maximum concentration of 4-CMC (500 μM) elicited an increase in $[Ca^{2+}]_i$ while control Flp-In 293 cells did not respond to 4-CMC challenge (black trace). Average (± SE) 4-CMC concentration-response relationships are shown in Figure 2B. HEK-RyR1 cells exhibited an EC_{50} for 4-CMC of ~ 30 μM similar to that described previously for RyR1 expressed in skeletal muscle myotubes [35]. Exposure of HEK-RyR1 cells to caffeine also elicited robust elevations in $[Ca^{2+}]_i$ (Figure 2C; black trace and pooled data in Figure 2D). Notably, caffeine-induced $[Ca^{2+}]_i$ release was markedly attenuated by prior incubation with a high concentration of ryanodine (Figure 2C; red trace and pooled data Figure 2D). Taken together, these data demonstrate the stable expression of appropriately ER localized and functional RyR1 Ca^{2+} release channels in HEK-RyR1 cells.

NIH-PA Author Manuscript

NIH-PA Author Manuscript

NIH-PA Author Manuscript

3.2 Ca^{2+} dependency of channels monitored by "on-nucleus" patch-clamp in HEK-RyR1 cells

A series of experiments were designed to investigate if channel activity consistent with the expression of RyR1 could be recorded from nuclei isolated from HEK-RyR1 cells. RyR channels are biphasically regulated by cytosolic [Ca^{2+}] [5]. Therefore, we initially performed experiments to assess whether a rapid increase in [Ca^{2+}] on the cytosolic face of the nuclear membrane would activate a large conductance channel in nuclei from HEK-RyR1 cells. On-nucleus patch clamp recordings were performed as detailed in Methods. The pipette contained K^+ as the primary charge carrying cation, together with caged-Ca^{2+} and $CaCl_2$ to result in free [Ca^{2+}] calculated to be ~ 100 nM prior to photolysis of the cage. No channel activity was evident prior to exposure to UV irradiation. However, photolysis of caged-Ca^{2+} by brief exposure to high intensity UV light focused on the patch pipette, which increased the pipette [Ca^{2+}] to > 10 μM, resulted in the appearance of channel activity with high open probability (average P_o increased from 0 to 0.32 ± 0.08 in the 3 s post uncaging) and relatively large current amplitude (unitary current magnitude at +40 mV = 30.2 ± 3.6 pA, resulting in a chord conductance of ~750 pS; Figure 3A and expanded time scale in Figure 3B). No evidence of prominent sub-conductance states were observed, which are sometimes reported when RyR1 channels are reconstituted in bilayers [36–38]. Similar pipette flash photolysis of caged-Ca^{2+} did not evoke channel activity in control Flp-In 293 cells (data not shown). These data indicate the presence of a Ca^{2+} activated K^+ permeable channel with a large single channel conductance, consistent with the presence of RyR1 in the outer nuclear membrane/ER of HEK-RYR1 cells.

To investigate the Ca^{2+} dependence of the channel activity in HEK-RyR1 cell nuclei in more detail, experiments were performed at varying [Ca^{2+}] in the pipette solution. In contrast to pipette solutions containing 100 nM Ca^{2+} where no activity was evident (Figure 3A), exposure to 1 μM Ca^{2+} resulted in the appearance of activity with a mean open probability (P_0) of ~0.04% (Figure 4A and C). In nuclear patches exposed to 100 μM Ca^{2+} the P_o significantly increased, achieving a mean P_o of ~0.36% (Figure 4B and C). Analysis of the kinetics of the channel activity revealed that the mean open time of the channel was not altered by increasing Ca^{2+}, however the mean closed time was significantly decreased (Figure 4D). As such, all-points histograms of open and closed times were best fitted by single exponential functions and revealed that the time constant for channel opening (τ_0) was not significantly altered by increasing [Ca^{2+}] from 1– 100 μM, while the time constant for channel closing (τ_c) was reduced ~10-fold.

3.3 Conductance of channels monitored by "on-nucleus" patch-clamp in HEK-RyR1 cells

RyR's, like IP_3R, assemble to form large conductance, cation-selective channels with permeability for monovalent and divalent ions [5]. These properties have been studied extensively in bilayers and consequently experiments were performed to ascertain whether the channels observed in HEK-RyR1 nuclear patches had similar conductance and permeability characteristics to those established for RyR channels incorporated into planar lipid bilayers. Current versus voltage relationships were generated in the presence of 1 μM pipette Ca^{2+} with equimolar concentrations of either Cs^+ or K^+ as the permeant ion (250 mM pipette:bath). Figure 5A (K^+) and B (Cs^+) show representative 3s sweeps of channel

NIH-PA Author Manuscript

NIH-PA Author Manuscript

NIH-PA Author Manuscript

activity at the indicated pipette potential and Figure 5C illustrates the average current versus voltage relationships generated from these experiments. The recorded channel activity exhibited no discernable voltage dependency and the current versus voltage relationships were ohmic, yielding a slope conductance of 745 ± 18 pS with K^+ as the permeant ion and 454 ± 17 pS with the channel conducting Cs^+. The absolute magnitude of the conductance in each case, and the decrease in conductance observed when Cs^+ is the charge carrier is entirely consistent with the characteristics of RyR channels reported in bilayer studies [5, 39–41].

3.4 Pharmacology of channels monitored by “on-nucleus” patch-clamp in HEK-RyR1 cells

To further characterize the identity of the channel activity in HEK-RyR1 nuclei, experiments were performed to ascertain whether the single channel activity was subject to modulation by pharmacological agents that either directly affect RyR channel activity or alter Ca^{2+} release in a manner dependent on RyR channels. Initial experiments were performed with caffeine, an established activator of Ca^{2+} release through RyR [42, 43]. As shown in the representative sweeps in Figure 6A, low channel activity was observed in the presence of 1 μM Ca^{2+} in the patch pipette which then increased, after a short latency, following exposure to 10 mM caffeine. Specifically, mean channel P_o increased from ~0.04% in control to ~0.35% in the presence of 10 mM caffeine (Figure 6A and average pooled time course in Figure 6B). Analysis of the kinetics of the channel activity showed that exposure to caffeine, in a manner similar to the effects of raising Ca^{2+}, did not markedly alter the mean open dwell time of the channel, but significantly reduced the mean closed time (Figure 6C). Again, frequency distributions of events were best fit by single exponential functions and revealed that caffeine significantly reduced τ_c without effects on τ_o (Figure 6D). Thus, the major effect of caffeine on Ca^{2+} activated channels in HEK-RyR1 cells was to facilitate channel opening by destabilizing a closed state of the channel. A similar kinetic scheme, whereby caffeine sensitizes RyR to Ca^{2+} by destabilizing the closed state of the channel was proposed previously based on bilayer measurements of RyR2 channels reconstituted in planar lipid bilayers [43].

A defining characteristic of RyRs is that exposure to the plant alkaloid ryanodine has complex effects on the biophysical properties of channel activity [43, 44]. For example, while low nanomolar concentrations of ryanodine increase the frequency of channel openings and high concentrations (>100 μM) block channel activity, intermediate concentrations (~1–10 μM) have the “signature” effect of locking the channel into a long-lived sub-conductance state [5]. The long-lived sub-conductance state is thought to occur as a consequence of ryanodine binding to a high affinity open-state of the channel that is close enough to the pore as to alter the ion permeation pathway. As shown in the representative trace in Figure 7, bath superfusion of nuclei exposed to 100 μM Ca^{2+} in the patch pipette with 10 μM ryanodine resulted in the abrupt appearance of a sub-conductance state essentially locked in the open state. Specifically, the single channel current magnitude recorded at +40 mV was reduced from 30.2 pA to 12.1 ± 0.5 pA in the presence of ryanodine, representing a 60% decrease in single channel K^+ conductance (745 pS to 292.7 ± 3.1 pS).

NIH-PA Author Manuscript

NIH-PA Author Manuscript

NIH-PA Author Manuscript

Having established RyR1 channel activity in nuclei of HEK-RyR1 cells, we next performed a series of experiments to assess whether this activity was modulated by agents suggested to alter RyR1 channels. For example, nicotinic acid adenine dinucleotide phosphate (NAADP) is a potent Ca^{2+} releasing substance in a variety of mammalian cells whose target has not been unequivocally established. A promising current candidate receptor is the Two Pore Channel (TPC) protein family, though evidence from lymphocytes and pancreatic acinar cells have suggested that NAADP may promote Ca^{2+} release through activation of RyR channels [45–47]. However, in HEK-RyR1 nuclei, RyR1 channel activity recorded in 1 μM Ca^{2+} was not significantly altered by either 30 nM or 1 μM NAADP (Figure 8). Cyclic ADP ribose (cADPr) has prominent effects on Ca^{2+} signaling in non-muscle cells that have been attributed to activation of RyR channels [48]. However, 100μM cADPr failed to significantly alter RyR1 channel activity recorded in the presence 1 μM Ca^{2+} (Figure 8). Finally, dantrolene reduces RyR1-dependent Ca^{2+} release in skeletal muscle, but does not directly inhibit RyR1 channels incorporated in bilayers [49, 50]. Consistent with this, dantrolene (25 μM) did not significantly alter single RyR1 channel activity in HEK-RyR1 nuclei (Figure 8).

4. Discussion

In this study, we provide the first biophysical and pharmacological characterization of single RyR1 channels localized to a native intracellular membrane using the “on nucleus” configuration of the patch clamp technique. The biophysical properties of RyR1 have previously been exclusively studied in planar lipid bilayers. However, the endogenous properties of the channels could potentially be altered by the purification and reconstitution procedures conducted when performing bilayer experiments. On the other hand, on-nucleus patch clamp recordings of IP_3Rs have yielded a wealth of fundamental information regarding the gating and regulation of these channels in native intracellular membranes [20–22]. Thus, we reasoned that RyR should be similarly amenable to this experimental approach.

A cornerstone for interpreting all single channel data is to establish a weight of evidence that provides a compelling argument that the single channel measurements presented indeed reflect the activity of the channel of interest. Several lines of evidence strongly support the contention that the single channel currents reported in this study resulted from the expression of RyR1. First, RyR1 channels were expressed in an essentially *null* background. As an expression platform, Flp-In 293 cells were utilized. We confirmed by immunoblotting and immunohistochemistry that these cells lack RyR1, prior to ectopic expression. Moreover, Ca^{2+} release in response to the RyR1 agonist 4-CMC was refractory. In contrast, following stable expression of RyR1, immunoblots demonstrated the expression of a RyR1-immunoreeactive band of appropriate molecular weight (<500 kDa) in HEK-RyR1 cells. Furthermore, the protein was clearly localized to perinuclear structures and exhibited a striking reticular distribution consistent with ER nuclear membrane and localization. Ca^{2+} release was evoked in a concentration-dependent manner by 4-CMC. Release could also be induced by caffeine and inhibited by high concentrations of ryanodine. In total, these data are consistent with the expression of functional RyR1 channels within the ER of HEK-RYR1 cells and establish this cell line as an appropriate system to study the channel.

NIH-PA Author Manuscript

NIH-PA Author Manuscript

NIH-PA Author Manuscript

In contrast to the parental Flp-In 293 cells, where RyR1 channel activity was never observed, nuclei prepared from HEK-RyR1 consistently exhibited large conductance cation channels under appropriate activating conditions. Importantly, the single channel properties of these channels were consistent with known characteristics of RyR1 channels. The channel activity measured in HEK-RyR1 nuclei was ohmic and characterized by a large unitary conductance of ~ 750 pS in symmetrical 250 mM KCl. Notably, the unitary conductance of the channel was indistinguishable from that reported under similar conditions for cardiac and skeletal RyRs reconstituted in bilayers [5, 39]. Moreover, the unitary conductance was substantially larger than that reported for IP_3R recorded under similar conditions [6]. Further, the decrease in unitary conductance to ~428 pS measured in symmetrical CsCl reflects the reported permeability ratio for group 1 alkali metals through RyR in bilayers recorded under very similar conditions. Specifically, Li^+ Na^+ and K^+ permeate RyR equally well, whereas in comparison the permeability ratio for Cs^+ is 0.61 [40, 41]. The reduced permeability of RyR to Cs^+ is a signature characteristic of the channel and is thought to reflect a higher affinity of Cs^+ for components of the ion permeation pathway. Thus, the unitary conductance and relative K^+/Cs^+ permeation properties of the channels recorded from nuclei of HEK-RyR1 cells correspond well with previous measurements of purified RyR1 channels recorded in planar lipid bilayers.

An increase in cytoplasmic $[Ca^{2+}]$ is a principal activator of RyRs. Therefore, our demonstration that the P_o of channels recorded from HEK-RyR1 nuclei was markedly increased ~10-fold by elevating cytoplasmic Ca^{2+} from 1 μM to 100 μM $[Ca^{2+}]$ is also consistent with their identity as RyR1 channels. The dynamic nature of the activation by Ca^{2+} is most clearly illustrated by our demonstration in Figure 3 that channel activity was increased rapidly following UV flash photolysis of caged Ca^{2+}. Previous bilayer and ryanodine binding studies have established that RyR channel activity is biphasically regulated by $[Ca^{2+}]$ with micromolar concentrations causing activation and millimolar concentrations resulting in channel inhibition [5, 18, 39, 51, 52]. Thus, while experiments here were not performed at higher $[Ca^{2+}]$, a further $[Ca^{2+}]$ elevation would be expected to reduce P_o in this system. The distribution of open and closed times was well fit by a single exponential function, reflecting a simple, direct transition between two kinetically distinct states. Further, the increase in P_o as $[Ca^{2+}]$ increased was accomplished by a marked decrease in the time constant describing the closed time with little effect on the open time constant. These results indicate that Ca^{2+} functions to destabilize the closed state, and thus, facilitate the transition from closed to opening. While gating schemes generated from bilayer data are generally more complicated and typically involve multiple closed and open states of the channel, a similar kinetic mechanism whereby Ca^{2+} solely interacts with a closed state of RyR2 to increase the rate of channel opening was previously proposed [51].

Of interest, similar general mechanisms are thought to result in activation of IP_3R. For example, activators of IP_3Rs, principally IP_3 and Ca^{2+}, also increase P_o predominately by increasing the opening rate by destabilizing a closed state of the channel. However, the gating of IP_3R channels differ somewhat to that observed for RyR1 in the current study. Specifically, IP_3R exhibit a form of “modal gating” such that increasing agonist concentration augments a “bursting” mode of activity. Within bursts, mean channel open and closed times are not altered by stimuli, but agonist-induced destabilization of a long-

NIH-PA Author Manuscript

NIH-PA Author Manuscript

NIH-PA Author Manuscript

lived closed state results in increased P_o due to increases in burst duration and frequency [32, 53, 54]. Although we found no evidence of RyR1 bursting activity in nuclei of HEK-RyR1 cells, this form of gating has been reported for RyR2 channels in bilayers [43]. Our studies provide no insight into these differences, but they may reflect the different RyR isoforms, approaches and cellular contexts used in these studies [5].

A further series of experiments were performed to confirm that channels recorded from HEK-RyR1 nuclei were modulated in a predictable way by known RyR channel ligands. In particular, we investigated the effects of caffeine and ryanodine as modulation of channel activity by these agents are regarded as defining features of RyR channels [42–44]. Consistent with its documented effect to increase the sensitivity of RyR to activating Ca^{2+}, caffeine exposure at sub maximal [Ca^{2+}], rapidly increased channel P_o as a result of an increase in the rate of channel opening. Similarly, application of ryanodine resulted in the appearance of a characteristic long-lived sub-conductance state. The increase in channel open probability to unity concurrent with a reduction in single channel current amplitude are consistent with the effects of ryanodine on RyR channels in bilayer recordings, which exhibit a similar reduction in current amplitude (40–60%) and increase in P_o following ryanodine modification. As noted previously, there is no consensus in the literature as to whether the putative second messengers cADP ribose and NAADP, or the therapeutic agent dantrolene, exert *direct* effects on RyR channels. While these agents have been shown to influence Ca^{2+} release in intact cells, bilayer studies have largely failed to demonstrate direct effects of these agents on reconstituted RyR channels. Consistent with these findings, we found that RyR1 channel activity in nuclei of HEK-RyR1 cells was unaltered by cADP ribose, NAADP or dantrolene, indicating that these agents are unlikely to directly modulate RyR1 channels. However, we cannot rule out that these agents may act on RyR2/3 channels or indirectly regulate RyR1 activity through RyR1 associated accessory proteins that are not present in the HEK-RyR1 nuclei system.

The conductance/permeation properties, Ca^{2+} activation, pharmacology, and ryanodine modification of channels reported in this study provide compelling evidence that this activity reflects RyR1 channel behavior within native nuclear membranes. In spite of these similarities, a striking difference in channel gating was observed for RyR1 channels in native nuclear membranes compared to that observed for purified RyR1 channels reconstituted in artificial bilayers. Specifically, unlike RyR1 bilayer recordings, RyR1 channels in native nuclear membranes exhibit very clear open and closed states, no subconductance behavior, and simple gating transitions between single open and closed states without evidence for additional kinetically distinct states or bursting behavior. Channel activity consisted of well-resolved, discrete openings to a single current amplitude, likely representing the full open state of the channel. The absence of any marked sub-conductance states in these recordings is in contrast to many bilayer studies, which often report the existence of multiple partial open states [36]. The appearance of sub-conductance states may reflect disruption of the channel during purification or the absence of essential factors required for coordinated gating of the channel following bilayer incorporation. Of note, FKBP12 is reported to facilitate the coordinated gating of RyR1 channels to the full open state [55] and the expression of this protein was confirmed in HEK-RyR1 cells. As a

NIH-PA Author Manuscript

NIH-PA Author Manuscript

NIH-PA Author Manuscript

result, RyR1 channel gating in native membranes is more regular and stationary than that observed following purification and incorporation of the channel into artificial bilayers. While muscle-specific regulatory proteins may be absent from the HEK-RYR1 expression system, the gating characteristics of RyR1 reported here likely reflect the fundamental core biophysical properties of the RyR1 tetramer within a native membrane. This increased stability in gating observed in native membranes may be particularly important for studies designed to characterize the functional implications of endogenous regulators or disease mutations that may act by altering critical inter-domain interactions within the core tetrameric RyR channel complex.

In summary, these data provide strong biophysical and pharmacological evidence that recordings of RyR single channel activity can be accomplished in nuclei expressing RyRs. Further, since burgeoning numbers of RyR mutations are associated with multiple distinct disease states [56, 57], this report provides a powerful experimental paradigm to characterize the properties of these mutant channels, as well as the molecular determinants of RyR channel modulation, within the context in a native cellular membrane compartment and with minimal disruption of the channel complex.

Acknowledgments

This work also was supported by NIH grants DE019245/DE014756 to DIY and AR053349 to RTD. The Authors wish to thank members of the Yule and Dirksen labs for many helpful discussions throughout the period of this work

Abbreviations

RyR1	Ryanodine receptor type 1
IP_3R	Inositol1,4,5-trisphosphate Receptor
NAADP	Nicotinic acid adenine dinucleotide phosphate
cADPr	cyclic ADP ribose
ER	Endoplasmic Reticulum
SR	Sarcoplasmic reticulum

References

1. Berridge MJ, Lipp P, Bootman MD. The versatility and universality of calcium signalling. Nat Rev Mol Cell Biol. 2000; 1:11–21. [PubMed: 11413485]
2. I, Serysheva. Structure and Function of Calcium Release Channels. Academic Press; 2010.
3. Capes EM, Loaiza R, Valdivia HH. Ryanodine receptors. Skeletal muscle. 2011; 1:18. [PubMed: 21798098]
4. Lanner JT, Georgiou DK, Joshi AD, Hamilton SL. Ryanodine receptors: structure, expression, molecular details, and function in calcium release. Cold Spring Harbor perspectives in biology. 2010; 2:a003996. [PubMed: 20961976]
5. Fill M, Copello JA. Ryanodine receptor calcium release channels. Physiol Rev. 2002; 82:893–922. [PubMed: 12270947]
6. Foskett JK, White C, Cheung KH, Mak DO. Inositol trisphosphate receptor Ca2+ release channels. Physiol Rev. 2007; 87:593–658. [PubMed: 17429043]

NIH-PA Author Manuscript

NIH-PA Author Manuscript

NIH-PA Author Manuscript

7. Bosanac I, Alattia JR, Mal TK, Chan J, Talarico S, Tong FK, Tong KI, Yoshikawa F, Furuichi T, Iwai M, Michikawa T, Mikoshiba K, Ikura M. Structure of the inositol 1,4,5-trisphosphate receptor binding core in complex with its ligand. Nature. 2002; 420:696–700. [PubMed: 12442173]
8. Bosanac I, Michikawa T, Mikoshiba K, Ikura M. Structural insights into the regulatory mechanism of IP3 receptor. Biochimica et biophysica acta. 2004; 1742:89–102. [PubMed: 15590059]
9. Lobo PA, Van Petegem F. Crystal structures of the N-terminal domains of cardiac and skeletal muscle ryanodine receptors: insights into disease mutations. Structure. 2009; 17:1505–1514. [PubMed: 19913485]
10. Van Petegem F. Ryanodine receptors: structure and function. J Biol Chem. 2012; 287:31624–31632. [PubMed: 22822064]
11. Seo MD, Velamakanni S, Ishiyama N, Stathopulos PB, Rossi AM, Khan SA, Dale P, Li C, Ames JB, Ikura M, Taylor CW. Structural and functional conservation of key domains in InsP3 and ryanodine receptors. Nature. 2012; 483:108–112. [PubMed: 22286060]
12. Bezprozvanny I. The inositol 1,4,5-trisphosphate receptors. Cell Calcium. 2005; 38:261–272. [PubMed: 16102823]
13. Yule DI, Betzenhauser MJ, Joseph SK. Linking structure to function: Recent lessons from inositol 1,4,5-trisphosphate receptor mutagenesis. Cell Calcium. 2010; 47:469–479. [PubMed: 20510450]
14. Ivanova H, Vervliet T, Missiaen L, Parys JB, De Smedt H, Bultynck G. Inositol 1,4,5-trisphosphate receptor-isoform diversity in cell death and survival. Biochimica et biophysica acta. 2014
15. Clapham DE. Calcium signaling. Cell. 1995; 80:259–268. [PubMed: 7834745]
16. Bootman MD, Rietdorf K, Collins T, Walker S, Sanderson M. Ca2+-sensitive fluorescent dyes and intracellular Ca2+ imaging. Cold Spring Harbor protocols. 2013; 2013:83–99. [PubMed: 23378644]
17. Bezprozvanny I. Bilayer measurement of endoplasmic reticulum Ca2+ channels. Cold Spring Harbor protocols. 2013; 2013
18. Smith JS, Coronado R, Meissner G. Sarcoplasmic reticulum contains adenine nucleotide-activated calcium channels. Nature. 1985; 316:446–449. [PubMed: 2410798]
19. Bezprozvanny I, Watras J, Ehrlich BE. Bell-shaped calcium-response curves of Ins(1,4,5)P3- and calcium-gated channels from endoplasmic reticulum of cerebellum. Nature. 1991; 351:751–754. [PubMed: 1648178]
20. Dellis O, Dedos SG, Tovey SC, Taufiq UrR, Dubel SJ, Taylor CW. Ca2+ entry through plasma membrane IP3 receptors. Science. 2006; 313:229–233. [PubMed: 16840702]
21. Wagner LE 2nd, Joseph SK, Yule DI. Regulation of single inositol 1,4,5-trisphosphate receptor channel activity by protein kinase A phosphorylation. J Physiol. 2008; 586:3577–3596. [PubMed: 18535093]
22. Rosker C, Meur G, Taylor EJ, Taylor CW. Functional ryanodine receptors in the plasma membrane of RINm5F pancreatic beta-cells. J Biol Chem. 2009; 284:5186–5194. [PubMed: 19116207]
23. Stehno-Bittel L, Luckhoff A, Clapham DE. Calcium release from the nucleus by InsP3 receptor channels. Neuron. 1995; 14:163–167. [PubMed: 7530018]
24. Mak DO, Foskett JK. Single-channel inositol 1,4,5-trisphosphate receptor currents revealed by patch clamp of isolated Xenopus oocyte nuclei. J Biol Chem. 1994; 269:29375–29378. [PubMed: 7961913]
25. Mak DO, McBride S, Foskett JK. Inositol 1,4,5-trisphosphate [correction of tris-phosphate] activation of inositol trisphosphate [correction of tris-phosphate] receptor Ca2+ channel by ligand tuning of Ca2+ inhibition. Proc Natl Acad Sci U S A. 1998; 95:15821–15825. [PubMed: 9861054]
26. Mak DO, McBride S, Raghuram V, Yue Y, Joseph SK, Foskett JK. Single-channel properties in endoplasmic reticulum membrane of recombinant type 3 inositol trisphosphate receptor. J Gen Physiol. 2000; 115:241–256. [PubMed: 10694253]
27. Wagner LE 2nd, Yule DI. Differential regulation of the InsP(3) receptor type-1 and -2 single channel properties by InsP(3), Ca(2)(+) and ATP. J Physiol. 2012; 590:3245–3259. [PubMed: 22547632]

NIH-PA Author Manuscript

NIH-PA Author Manuscript

NIH-PA Author Manuscript

28. Alzayady KJ, Wagner LE 2nd, Chandrasekhar R, Monteagudo A, Godiska R, Tall GG, Joseph SK, Yule DI. Functional inositol 1,4,5-trisphosphate receptors assembled from concatenated homo- and heteromeric subunits. J Biol Chem. 2013; 288:29772–29784. [PubMed: 23955339]
29. Mak DO, Vais H, Cheung KH, Foskett JK. Patch-clamp electrophysiology of intracellular Ca2+ channels. Cold Spring Harbor protocols. 2013; 2013:787–797. [PubMed: 24003191]
30. Mak DO, McBride S, Foskett JK. ATP regulation of type 1 inositol 1,4,5-trisphosphate receptor channel gating by allosteric tuning of Ca(2+) activation. J Biol Chem. 1999; 274:22231–22237. [PubMed: 10428789]
31. Mak DO, McBride S, Foskett JK. Regulation by Ca2+ and inositol 1,4,5-trisphosphate (InsP3) of single recombinant type 3 InsP3 receptor channels. Ca2+ activation uniquely distinguishes types 1 and 3 insp3 receptors. J Gen Physiol. 2001; 117:435–446. [PubMed: 11331354]
32. Wagner LE, Yule DI. Differential regulation of the InsP3 receptor type-1 and -2 single channel properties by InsP3, Ca2+ and ATP. J Physiol. 2012; 590:3245–3259. [PubMed: 22547632]
33. Graves TK, Hinkle PM. Ca(2+)-induced Ca(2+) release in the pancreatic beta-cell: direct evidence of endoplasmic reticulum Ca(2+) release. Endocrinology. 2003; 144:3565–3574. [PubMed: 12865339]
34. Jacobson AR, Moe ST, Allen PD, Fessenden JD. Structural determinants of 4-chloro-m-cresol required for activation of ryanodine receptor type 1. Molecular pharmacology. 2006; 70:259–266. [PubMed: 16601083]
35. Fessenden JD, Wang Y, Moore RA, Chen SR, Allen PD, Pessah IN. Divergent functional properties of ryanodine receptor types 1 and 3 expressed in a myogenic cell line. Biophys J. 2000; 79:2509–2525. [PubMed: 11053126]
36. Liu QY, Lai FA, Rousseau E, Jones RV, Meissner G. Multiple conductance states of the purified calcium release channel complex from skeletal sarcoplasmic reticulum. Biophys J. 1989; 55:415–424. [PubMed: 2539209]
37. Smith JS, Imagawa T, Ma J, Fill M, Campbell KP, Coronado R. Purified ryanodine receptor from rabbit skeletal muscle is the calcium-release channel of sarcoplasmic reticulum. J Gen Physiol. 1988; 92:1–26. [PubMed: 2459298]
38. Marx SO, Ondrias K, Marks AR. Coupled gating between individual skeletal muscle Ca2+ release channels (ryanodine receptors). Science. 1998; 281:818–821. [PubMed: 9694652]
39. Meissner G. Ryanodine receptor/Ca2+ release channels and their regulation by endogenous effectors. Annual review of physiology. 1994; 56:485–508.
40. Lindsay AR, Manning SD, Williams AJ. Monovalent cation conductance in the ryanodine receptor-channel of sheep cardiac muscle sarcoplasmic reticulum. J Physiol. 1991; 439:463–480. [PubMed: 1716676]
41. Chen DP, Xu L, Tripathy A, Meissner G, Eisenberg B. Selectivity and permeation in calcium release channel of cardiac muscle: alkali metal ions. Biophys J. 1999; 76:1346–1366. [PubMed: 10049318]
42. Rousseau E, Meissner G. Single cardiac sarcoplasmic reticulum Ca2+-release channel: activation by caffeine. Am J Physiol. 1989; 256:H328–333. [PubMed: 2537030]
43. Sitsapesan R, Williams AJ. Mechanisms of caffeine activation of single calcium-release channels of sheep cardiac sarcoplasmic reticulum. J Physiol. 1990; 423:425–439. [PubMed: 2167363]
44. Rousseau E, Smith JS, Meissner G. Ryanodine modifies conductance and gating behavior of single Ca2+ release channel. Am J Physiol. 1987; 253:C364–368. [PubMed: 2443015]
45. Guse AH. Linking NAADP to ion channel activity: a unifying hypothesis. Science signaling. 2012; 5:pe18. [PubMed: 22534131]
46. Galione A, Evans AM, Ma J, Parrington J, Arredouani A, Cheng X, Zhu MX. The acid test: the discovery of two-pore channels (TPCs) as NAADP-gated endolysosomal Ca(2+) release channels. Pflugers Arch. 2009; 458:869–876. [PubMed: 19475418]
47. Galione A, Petersen OH. The NAADP receptor: new receptors or new regulation? Molecular interventions. 2005; 5:73–79. [PubMed: 15821155]
48. Lee HC. Cyclic ADP-ribose and nicotinic acid adenine dinucleotide phosphate (NAADP) as messengers for calcium mobilization. J Biol Chem. 2012; 287:31633–31640. [PubMed: 22822066]

NIH-PA Author Manuscript

NIH-PA Author Manuscript

NIH-PA Author Manuscript

49. Szentesi P, Collet C, Sarkozi S, Szegedi C, Jona I, Jacquemond V, Kovacs L, Csernoch L. Effects of dantrolene on steps of excitation-contraction coupling in mammalian skeletal muscle fibers. J Gen Physiol. 2001; 118:355–375. [PubMed: 11585849]
50. Cherednichenko G, Ward CW, Feng W, Cabrales E, Michaelson L, Samso M, Lopez JR, Allen PD, Pessah IN. Enhanced excitation-coupled calcium entry in myotubes expressing malignant hyperthermia mutation R163C is attenuated by dantrolene. Molecular pharmacology. 2008; 73:1203–1212. [PubMed: 18171728]
51. Ashley RH, Williams AJ. Divalent cation activation and inhibition of single calcium release channels from sheep cardiac sarcoplasmic reticulum. J Gen Physiol. 1990; 95:981–1005. [PubMed: 2163436]
52. Smith JS, Coronado R, Meissner G. Single channel measurements of the calcium release channel from skeletal muscle sarcoplasmic reticulum. Activation by Ca2+ and ATP and modulation by Mg2+ J Gen Physiol. 1986; 88:573–588. [PubMed: 2431098]
53. Ionescu L, White C, Cheung KH, Shuai J, Parker I, Pearson JE, Foskett JK, Mak DO. Mode Switching Is the Major Mechanism of Ligand Regulation of InsP3 Receptor Calcium Release Channels. J Gen Physiol. 2007; 130:631–645. [PubMed: 17998395]
54. Siekmann I, Wagner LE 2nd, Yule D, Crampin EJ, Sneyd J. A Kinetic Model for type I and II IP3R accounting for mode changes. Biophys J. 2012; 103:658–668. [PubMed: 22947927]
55. Brillantes AB, Ondrias K, Scott A, Kobrinsky E, Ondriasova E, Moschella MC, Jayaraman T, Landers M, Ehrlich BE, Marks AR. Stabilization of calcium release channel (ryanodine receptor) function by FK506-binding protein. Cell. 1994; 77:513–523. [PubMed: 7514503]
56. Wei L, Dirksen RT. Ryanodinopathies: RyR-Linked Muscle Diseases. Current topics in membranes. 2010; 66C:139–167. [PubMed: 22353479]
57. Betzenhauser MJ, Marks AR. Ryanodine receptor channelopathies. Pflugers Arch. 2010; 460:467–480. [PubMed: 20179962]

NIH-PA Author Manuscript

NIH-PA Author Manuscript

NIH-PA Author Manuscript

Research Highlights

- On-nucleus patch clamp recording were performed in cells expressing Ryanodine Receptor 1.
- Single channel recordings were obtained with biophysical and pharmacological properties consistent with RyR1 activity in a native membrane.
- This experimental platform will be useful for the biophysical characterization of modulation of RyR activity and disease associated RyR mutants.

NIH-PA Author Manuscript
NIH-PA Author Manuscript
NIH-PA Author Manuscript

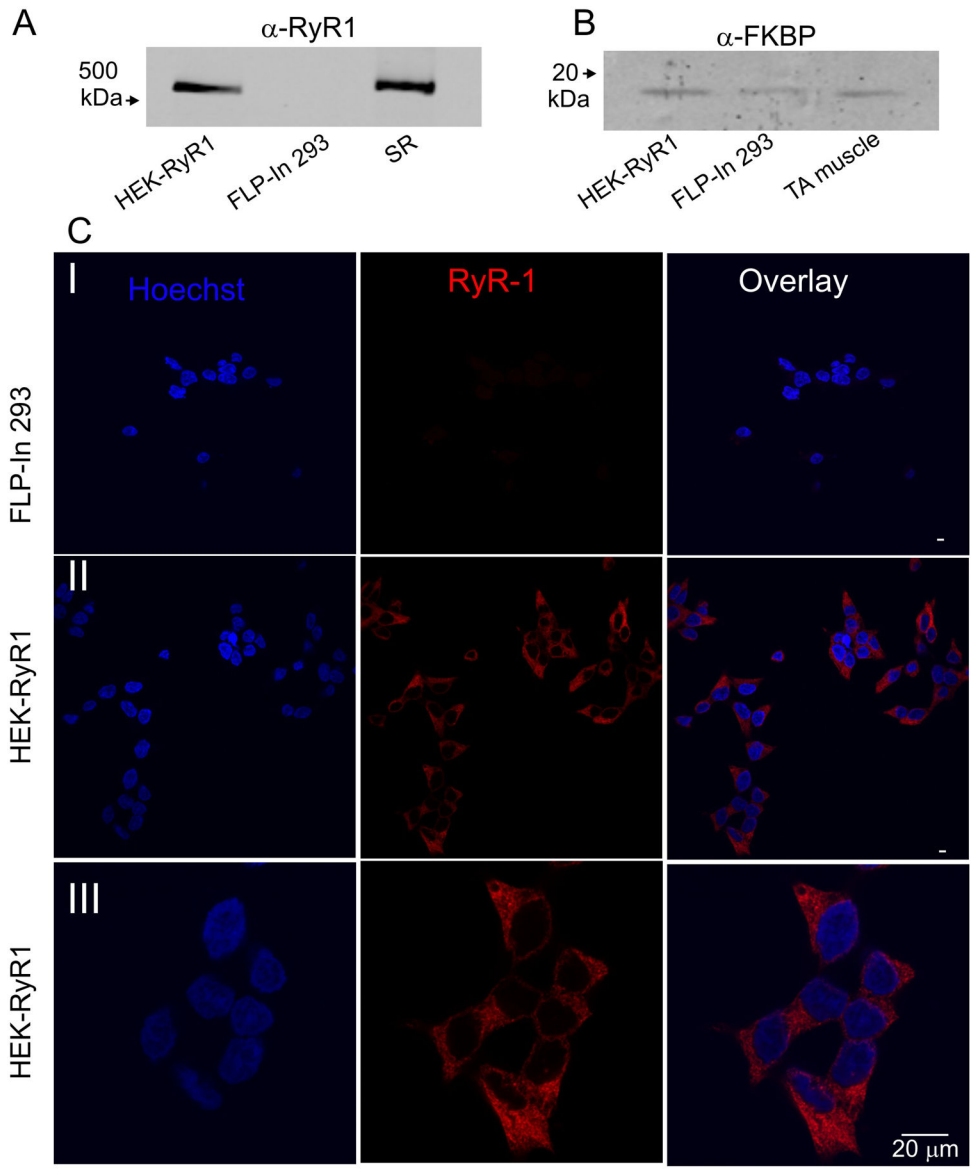

Figure 1. RyR1 and FKBP expression in RyR1 stable Flp-In cells

A) Representative western blot analysis of 10 μg each of HEK-RyR1 and control Flp-In 293 cell lysates probed with anti-RyR antibody. A sarcoplasmic reticulum (SR) preparation (5 μg) from mouse skeletal muscle was used as a positive control. B) Representative western blot analysis of 10 μg each of HEK-RyR1 and control Flp-In 293 cell lysates probed with anti-FKBP (1:100) antibody. A tibialis anterior (TA) mouse muscle homogenate preparation (10 μg) was used as a positive control for FKBP12. C) Control Flp-In 293 cells (Panel I) and HEK-RyR1 cells (Panels II and III) showing Hoechst 34580 nuclear staining alone (*left*), RyR1 immunostaining alone (*middle*) and overlay (*right*).

NIH-PA Author Manuscript

NIH-PA Author Manuscript

NIH-PA Author Manuscript

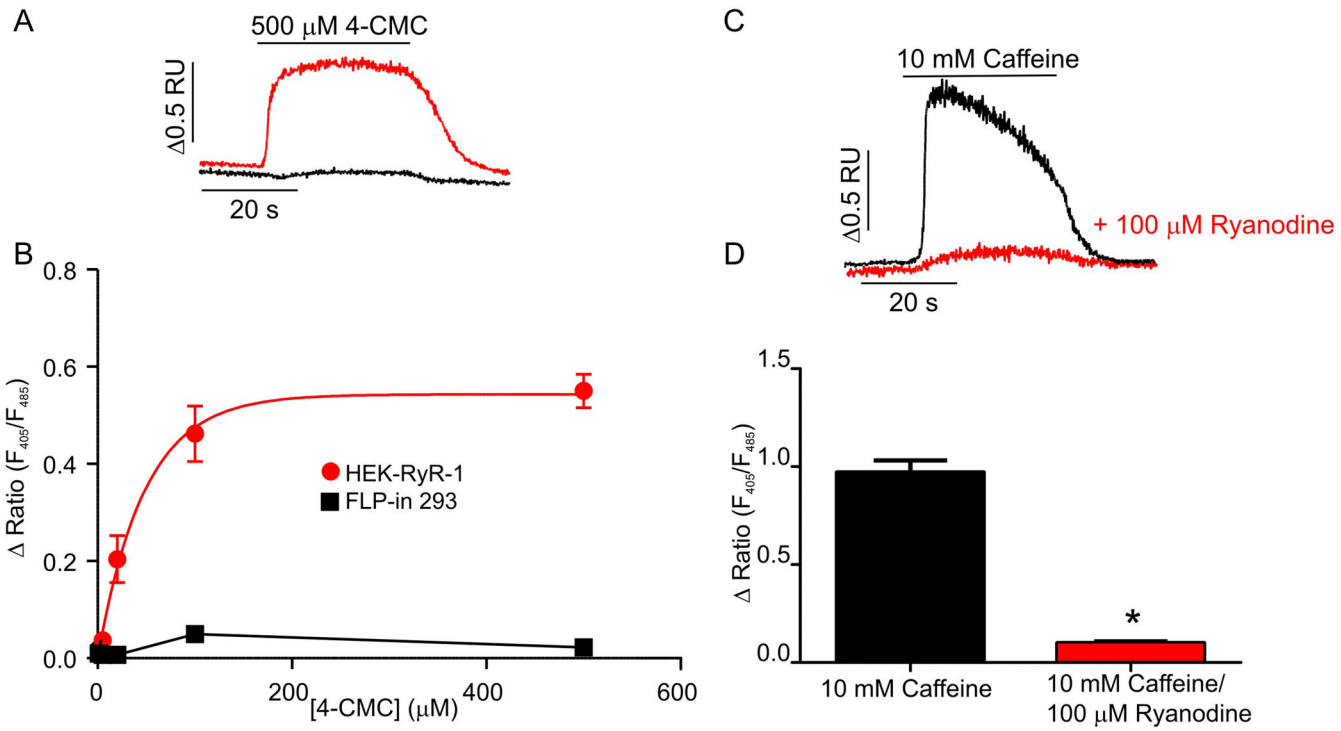

Figure 2. RyR1 Ca^{2+} release channel function in stable HEK-RyR1 cells

(A) Representative indo-1 ratio traces obtained from HEK-RyR1 cells (red) and control (black) Flp-In 293 cells during application of 500 μM 4-CMC. (B) Average (± SE) 4-CMC concentration-response curves for RyR1 stably expressing (red) and control (black) Flp-In 293 cells. (C) Representative indo-1 ratio traces obtained from HEK-RyR1 cells during application of 10 mM caffeine in the absence (black) and presence (red) of pretreatment with 100 μM ryanodine. (D) Average (± SE) response of HEK-RyR1 cells to 10 mM caffeine in the absence (black) and presence (red) of pretreatment with 100 μM ryanodine. *$p < 0.05$.

NIH-PA Author Manuscript

NIH-PA Author Manuscript

NIH-PA Author Manuscript

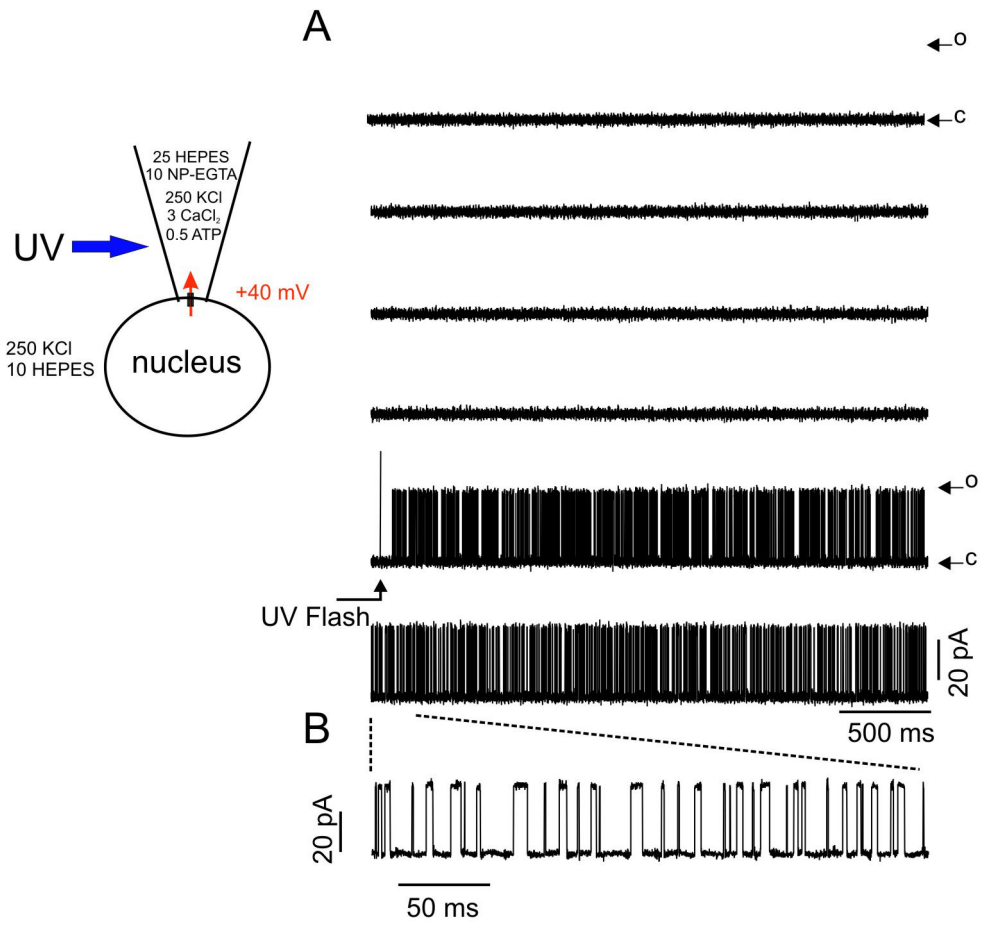

Figure 3. Uncaging [Ca^{2+}] in the patch pipette triggers single channel activity

The cartoon illustrates the voltage clamp and ionic conditions. Patch pipette contained (in mM): 250 KCl, 25 HEPES, 10 NP-EGTA, 3 $CaCl_2$, 0.5 Na-ATP. The holding potential was +40 mV. Free [Ca^{2+}] prior to UV flash was <100 nM. Upon UV photolysis, free [Ca^{2+}] increased to >10 μM. (*A)* Representative current traces of this and four other experiments displayed no channel activity prior to UV flash. Upon photolysis, following a short latency, channel activity increased markedly. Openings (O) from the closed state (*C*) are denoted by upward deflections. (*B)* Magnifying a 300 ms section of the trace allows better visualization of discrete openings and closings.

NIH-PA Author Manuscript

NIH-PA Author Manuscript

NIH-PA Author Manuscript

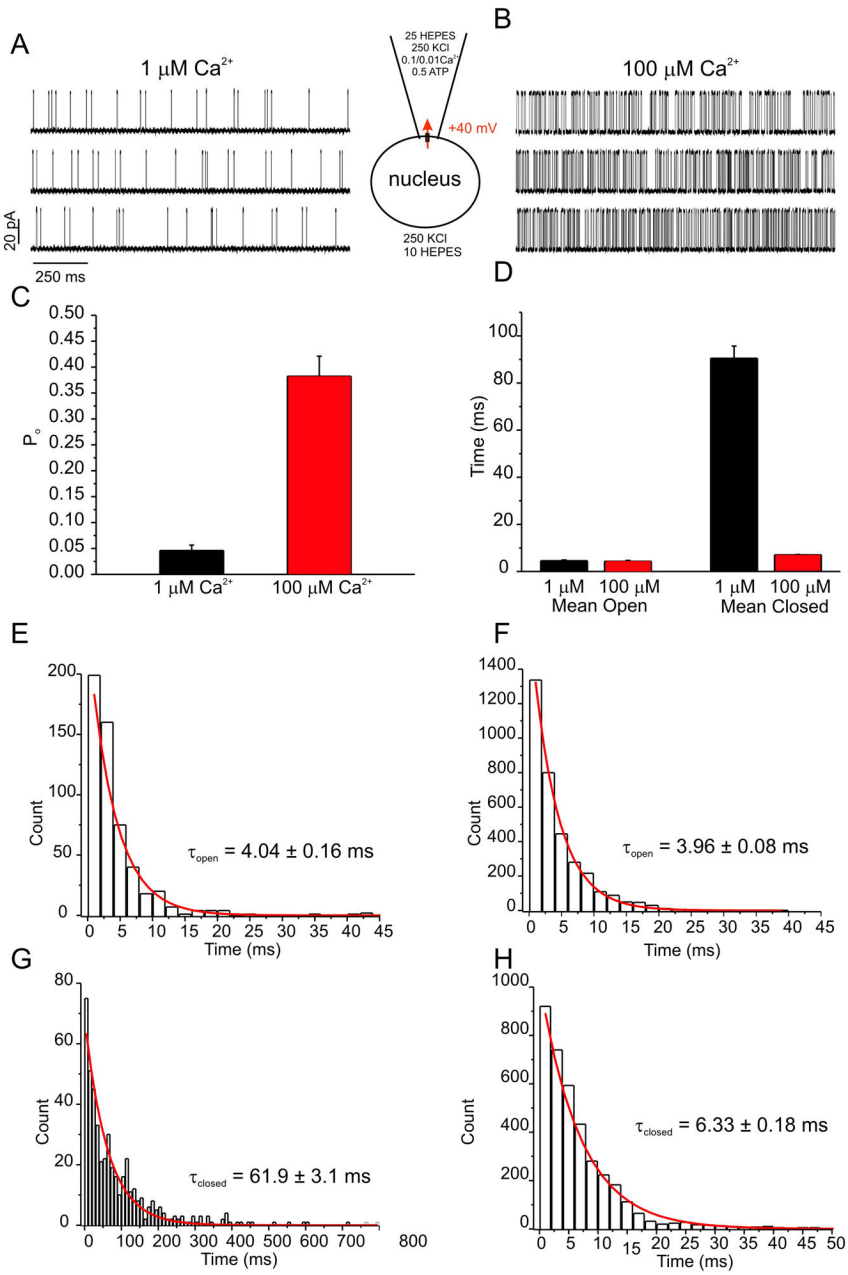

Figure 4. Increasing [Ca^{2+}] augments open probability through enhancing transition from a closed state

Representative current traces at +40 mV are shown for experiments with pipette solutions containing either 1 μM (*A*) or 100 μM (*B*) Ca^{2+}. (*C*) Increasing pipette [Ca^{2+}] from 1 μM (black bar) to 100 μM (red bar) increased average channel open probability from 0.04 to 0.36. (*D*) Mean (± SE) channel open (left) and closed (right) times in the presence of either 1 μM (black bars) or 100 μM (red bars) pipette [Ca^{2+}]. All points histograms for open (*E*, *F*) and closed times (*G*, *H*) were constructed for 1 μM (*E*, *G*) and 100 μM (*F*, *H*) [Ca^{2+}] and fitted with single exponential functions. Time constants for open channel dwell times were

unaltered, but τ_{closed} was 10 times longer in 1 μM Ca^{2+}. Thus, higher [Ca^{2+}] destabilized the closed state, thereby permitting faster transitions into the open state. *$p < 0.05$

NIH-PA Author Manuscript
NIH-PA Author Manuscript
NIH-PA Author Manuscript

NIH-PA Author Manuscript
NIH-PA Author Manuscript
NIH-PA Author Manuscript

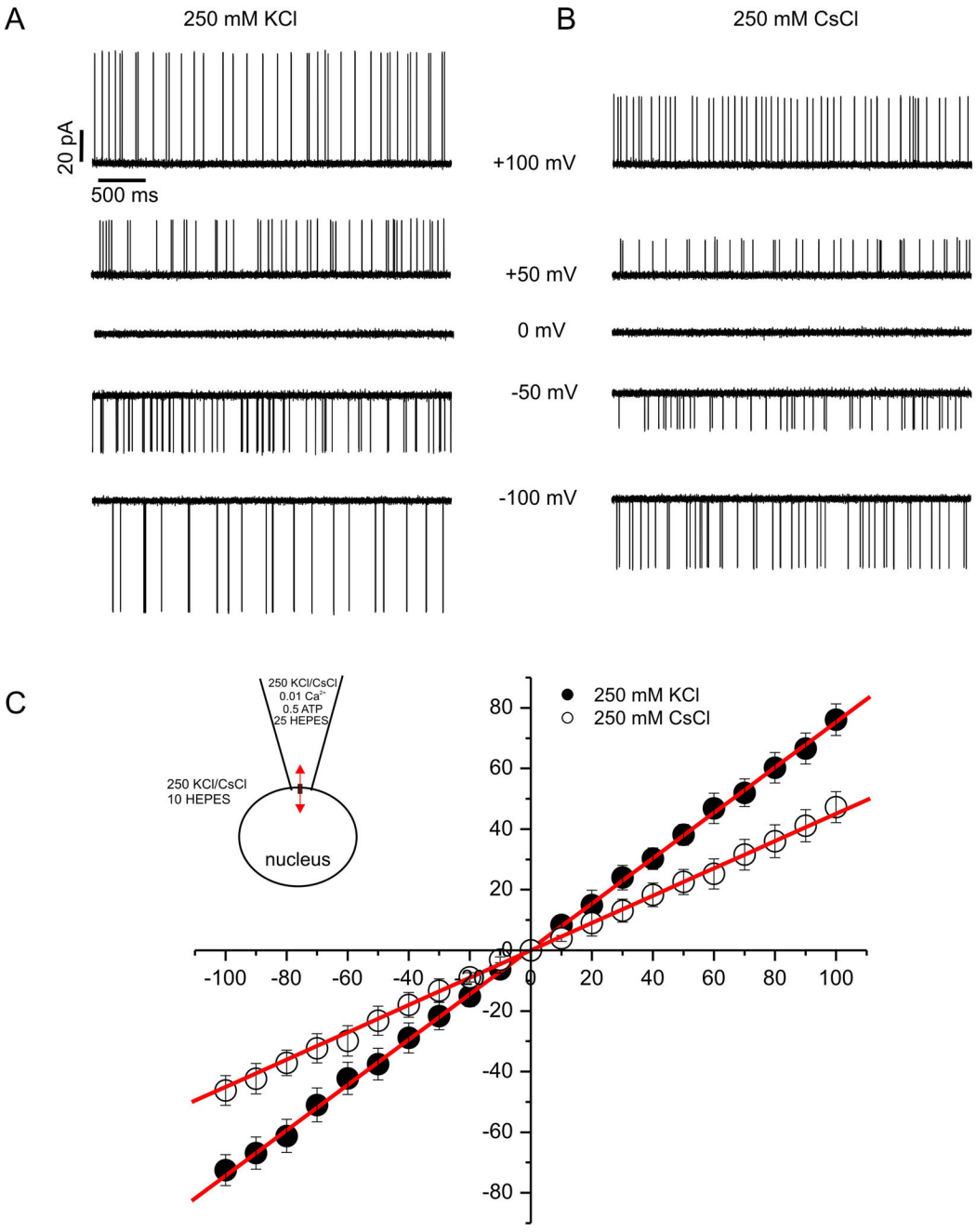

Figure 5. Ion selectivity favors potassium over cesium

Representative current traces at the voltages listed are shown with symmetrical K^+ (*A*) and Cs^+ (*B*) as the predominate charge carrying ions. (*C*) Average (± SE) current-voltage relationships were constructed for both KCl and CsCl experiments. Traces were obtained at test potentials between −100 mV and 100 mV in 10 mV increments. Data were fitted with linear functions and conductances were calculated from the slopes as described in Methods. Reversal potentials were unaltered. However, a profound decrease in the slope conductance from K^+ (745 ± 18 pS) to Cs^+ (454 ± 17 pS) as charge carrier was evident. Traces are representative examples of at least 4 other patches.

NIH-PA Author Manuscript

NIH-PA Author Manuscript

NIH-PA Author Manuscript

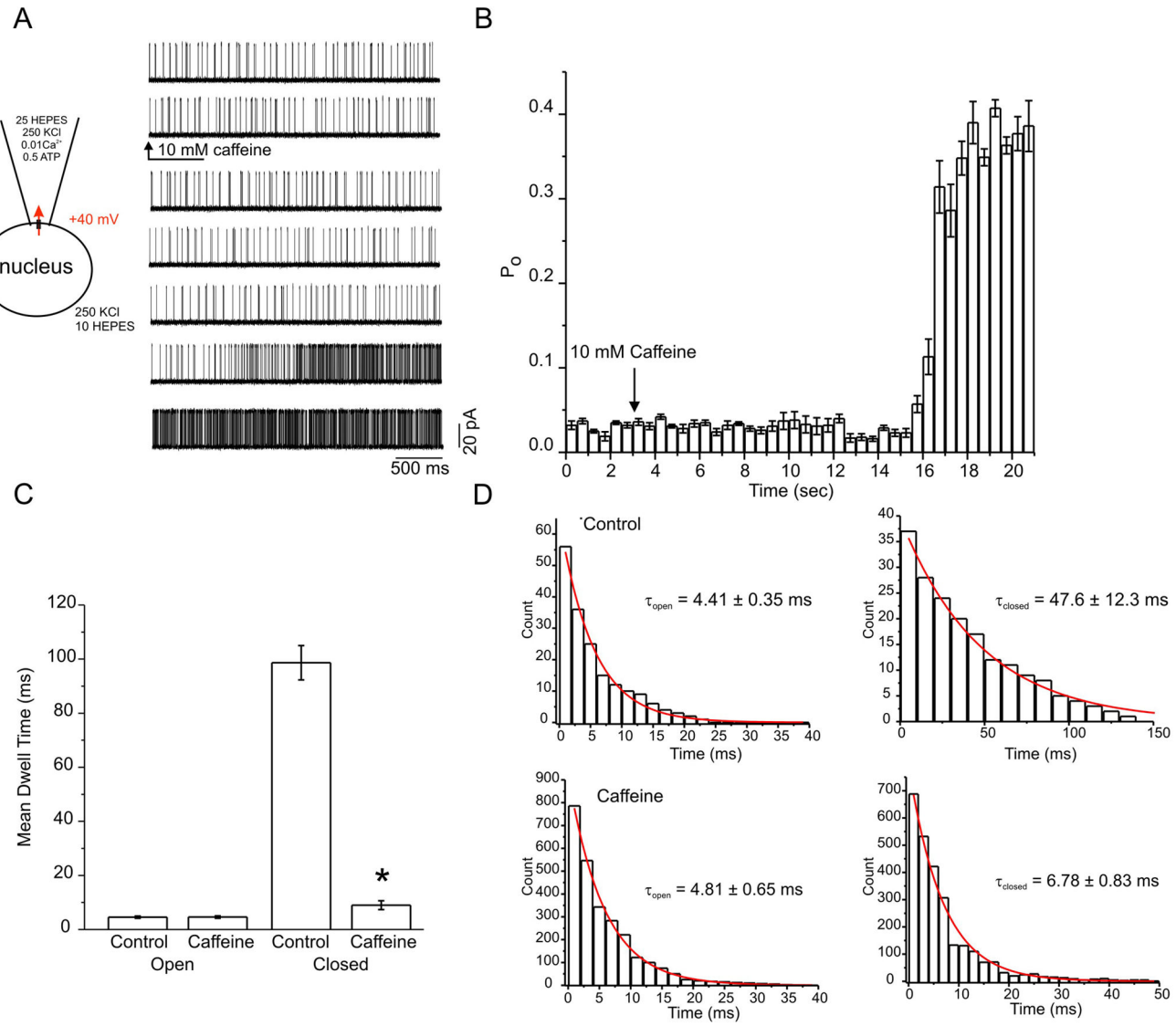

Figure 6. Caffeine shifts the Ca^{2+} dependence by promoting a transition out of a closed state

(*A*) Representative current traces are shown before and after addition of 10 mM caffeine. Caffeine increased channel open probability after a latency of several seconds. (*B*) Average (± SE) open probability histogram, binned in 500 ms increments, shows enhanced channel activity 12 seconds following the addition of 10 mM caffeine. (*C*) Bar charts constructed of mean (± SE) open (left) and closed (right) dwell times before and after addition of 10 mM caffeine. Only closed times were affected by caffeine. (*D*) Open (left) and closed (right) time histograms before and after the addition of 10 mM caffeine. Each distribution was well fitted with a single exponential. Time constants are inset into each graph. Open time constants were unaltered, while the closed time constant was reduced, in the presence of caffeine. Like Ca^{2+}, caffeine destabilizes the closed state, and thereby facilitates transitions into the open state. Traces are representative examples of at least 4 other patches.

NIH-PA Author Manuscript

NIH-PA Author Manuscript

NIH-PA Author Manuscript

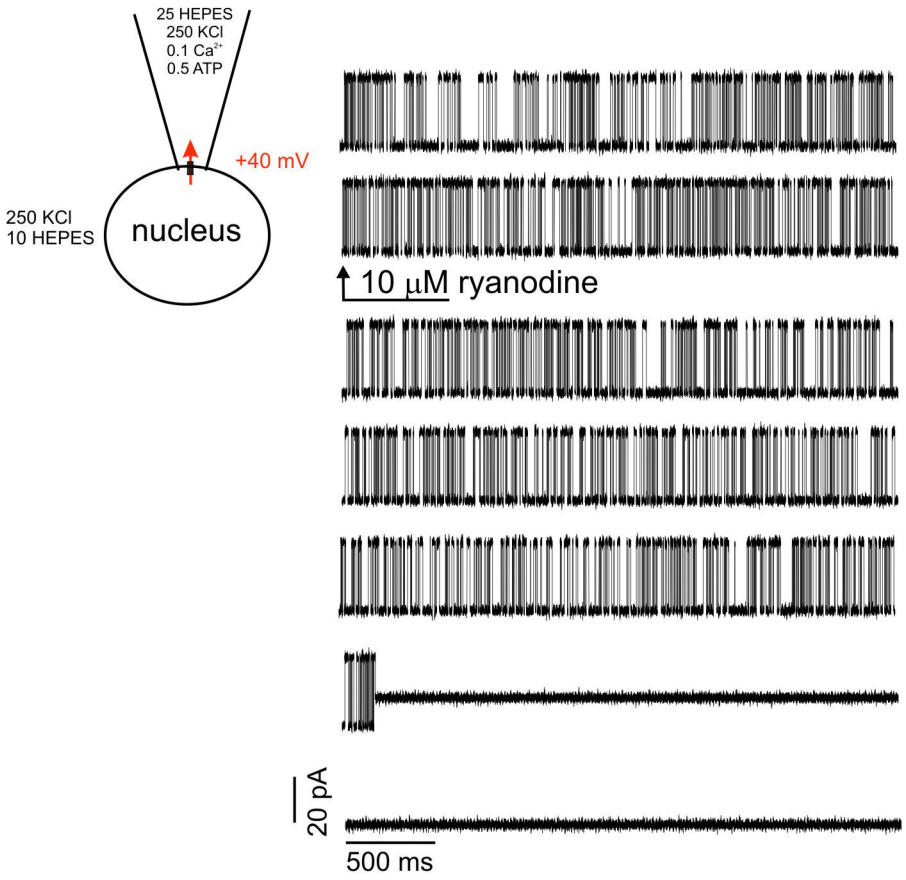

Figure 7. Ryanodine drives the channel into a long-lived sub-conductance state

Representative current traces are shown for recording in the presence of 100 μM Ca^{2+} immediately before and following perfusion of 10 μM ryanodine denoted by the arrow. Following ryanodine addition, the channel entered into a long-lived, sub-conducting state that did not transition back to the normal conductance state for several seconds, Traces are representative examples of at least 4 other patches.

NIH-PA Author Manuscript

NIH-PA Author Manuscript

NIH-PA Author Manuscript

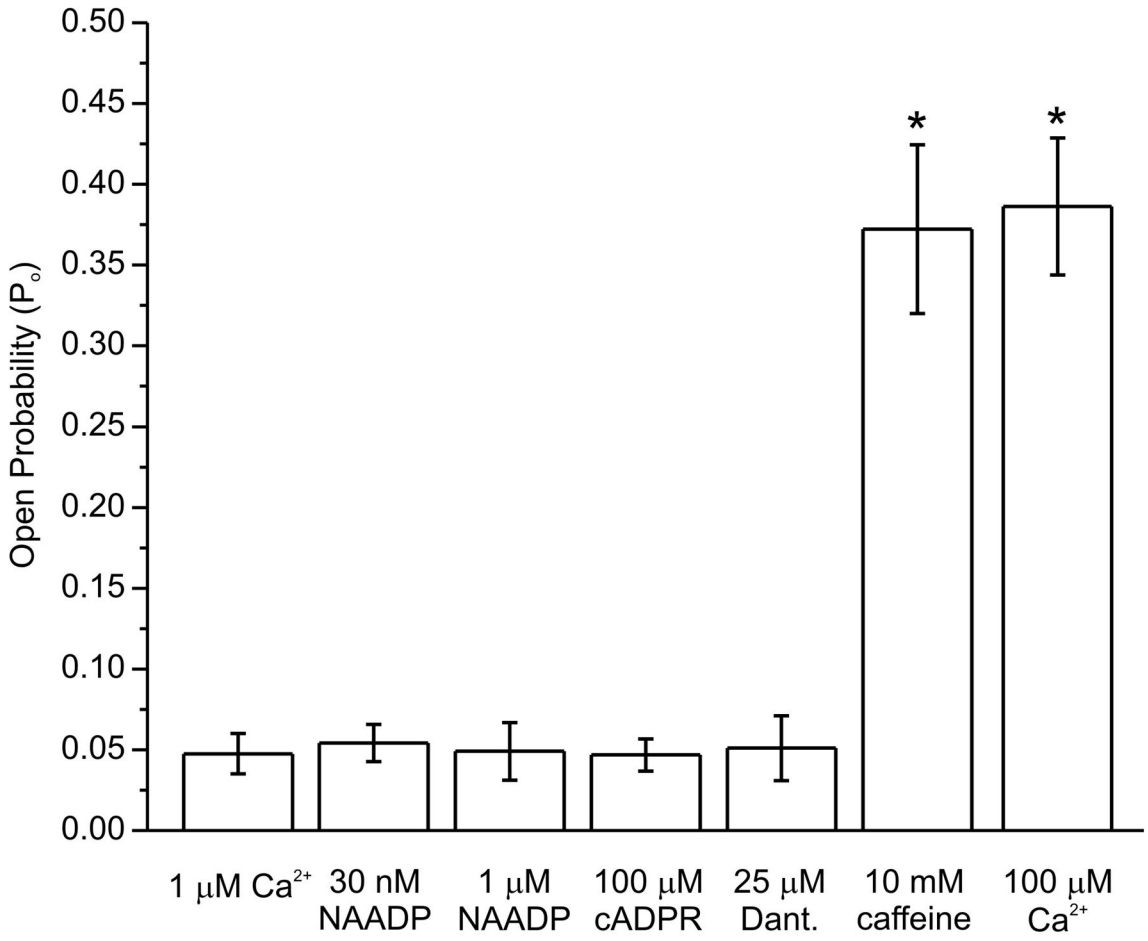

Figure 8. Effects of potential RyR modulators on open probability

Experiments were performed wit each compound listed in the presence of 1 μM Ca^{2+}, and separately in the presence of 100 μM Ca^{2+} to demonstrate maximal achievable P_o. Mean (± SE) open probabilities were calculated for each experiment. A bar chart was constructed for the grouped data ($n \geq 4$ for each condition) and plotted for each condition. Only caffeine and 100 μM Ca^{2+} had a significant effect on channel open probability in the presence of 1 μM Ca^{2+}.*$p < 0.05$.